JOURNAL OF APPLIED ELECTROCHEMISTRY 26 (1996) 1287–1294

Electrodeposition of gold in ammoniacal medium: influence of substrate and temperature

G. TREJO

Centro de Investigación y Desarrollo Tecnológico en Electroquímica CIDETEQ, Parque Tecnológico Sanfandila, Pedro Escobedo, Qro. Apdo. 064 C.P. 76700, Mexico D.F.

A. F. GIL, I. GONZÁLEZ*

Depto. de Química, Area de Electroquímica. Universidad Autónoma Metropolitana-Iztapalapa 09340, A.P. 55-534, 09340 México D.F., México

Received 18 December 1995; revised 28 March 1996

Gold electrodeposition was studied on glassy carbon and platinum electrodes from Au(I) ammoniacal solution. The current transients obtained from potential step perturbations, show a typical metallic nucleation growth controlled by diffusion. This process is influenced by adsorption of the different chemical species on the surface. Change in the type of nucleation and morphology of the deposit was observed when the nature of the substrate was changed. It was also found that increase in temperature produces modification of the nucleation mechanism.

1. Introduction

Electrodeposition and electrowinning of gold are normally performed using cyanide-based baths. However, these baths have the disadvantage of being strong pollutants because the cyanide ion is among the products obtained. For this reason, alternative nonpolluting baths have been sought (e.g., those based on thiourea, thiosulfate and ammonia). Unfortunately, research on the topic is scarce (cf. Rausepp and Allgood on the gold-thiourea complex [1]). Ammonia baths have been studied for leaching and electrodeposition of noble metals, such as silver [2–4], and good results have been reported by Meng for gold leaching [5]. Since the ammonia bath seems to be a good nonpolluting alternative for these processes, this bath has been selected in this work as a first choice. In a previous study, we reported the temperature effect on the electrodeposition of gold in the same medium [6].

The nucleation and growth processes during metal electrodeposition depend on several factors such as pH, complexing agents and potential. The temperature and the nature of the substrate are also important factors, and changes in either provokes modification of the type of nucleation obtained.

In this work the first steps of gold electrodeposition from a solution of gold tetrachloride are described. Voltammetric, potentiostatic and scanning electron microscopy (SEM) studies are undertaken to investigate the influence of the substrate and temperature on gold electrodeposition.

2. Experimental details

Gold was electrochemically deposited from a solution containing $H(AuCl_4) \cdot 3H_2O$ (Aldrich 99.99%) in 1 M NH_4Cl (Aldrich 99.99%). All chemicals were reagent grade and were prepared in distilled ultrafiltered water (18MΩcm resistivity). A PAR potentiostat–galvanostat (model 173), a PAR universal signal programmer (model 175) and a Nicolet oscilloscope (model 2090III) were used. The selected temperatures were imposed and maintained constant using a Cole Parmer constant temperature circulator.

The working electrodes were a glassy carbon disc (GC) and a platinum disc (Pt) of 0.07 cm^2 and 0.03 cm^2 geometric surface area, respectively. A saturated calomel electrode (SCE) (Tacussel) was used as reference, to which all potentials in this work are referred. A graphite rod was used as a counter electrode. The working electrodes were polished with 0.05 alumina (Buheler), and pretreated electrochemically in different solutions: the GC electrode in a solution containing 1×10^{-2} M $K_4Fe(CN)_6$ and 1 M KNO_3, and the platinum electrode with 1 M H_2SO_4. A conventional three electrode electrochemical cell with water jacket was used. All experiments were performed under a prepurified nitrogen atmosphere (Linde).

The surface morphology of the deposits was studied using SEM by means of a Jeol microscope (model DSM-5400LV). The surface chemical analysis was performed by energy dispersive spectrometry (EDS).

* Author to whom correspondence should be addressed.

0021-891X

3. Results and discussion

Prior to the electrochemical studies, a Pourbaix predominance diagram for the Au(III)/Au(I)/Au(0) system in ammoniacal medium was constructed from thermodynamic data [7–9] by considering the generalized chemical equilibria [10] for the following condition $pCl' = 0.0$, $pNH_3 = 0.0$ and $pAu' = 2.0$. The diagram was constructed using a graphical method [10–14] which is reported elsewhere [6]. From the diagram it may be concluded that, the generalized Au(III) species are not stable in solutions with a pH higher than 1.9 because they are reduced by water to Au(I). This reaction forms the complex $Au(NH_3)_2^+$ which is stable over a wide range of pH. As the experimental pH in the present studies is 2.8, the gold species considered is Au(I) as the ammonia complex.

3.1. *Substrate influence*

3.1.1. Voltammetric studies. Voltammetric studies were performed in the potential range −0.5 to +1.2 V at 25 °C on GC and Pt electrodes. Better reproducibility was obtained when the potential was swept in the anodic direction. Thus, all the experiments were started anodically from the open circuit potential. Typical cyclic voltammograms (CV) obtained for gold on GC (Fig. 1(a)) and Pt (Fig. 1(b)) are presented. It should be noted that the current scale for these CV is not the same, as the geometric surface area of GC is double that of the Pt electrode. Similar behaviour is obtained for both cases: the electroreduction process is accomplished in one step (peak Ic), associated with the reduction of Au(I) to Au(0). For GC, peak I_c appears at 0.36 V vs SCE, while on Pt this peak is shifted anodically, appearing at 0.59 V vs SCE. In both cases I_p (peak current) was found to be linear with $v^{1/2}$ (v = sweep rate), indicating diffusion control. Only one oxidation peak was observed (peak Ia) within the potential range studied.

A cross-over is observed between the anodic and cathodic scan only on GC (Fig. 1(a)). The potential for this crossover (E_{co}) is equal to that for the peak potential on the platinum electrode and is characteristic of nucleation processes.

The behaviour of the crossover potential (E_{co}) was studied by fixing the switching potential (E_λ) at the foot of the reduction peak (Fig. 2(a)). When E_λ is located at the foot of the reduction peak the number of formed nuclei is restricted and, in this potential range, electrodeposition in not diffusion controlled. Nuclei growth of gold on GC requires an overpotential provided in the forward potential scan; in the reverse scan, the deposition of gold is accomplished on the nuclei previously formed in the forward scan. For this reason, the cathodic current is higher.

It was found that the crossover potential (E_{co}) is independent of E_λ. From these studies and the

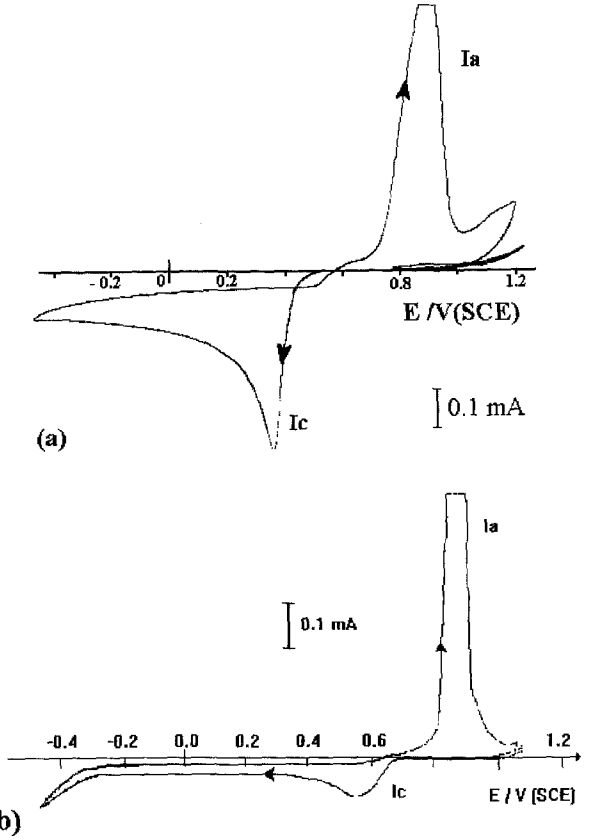

Fig. 1. Typical cyclic voltammograms for gold deposition from a solution containing 10^{-2} M $Au(NH_3)_2^+$ and 1 M NH_4Cl. v = 0.03 V s^{-1} and 25 °C on different substrate: (a) glassy carbon; (b) platinum.

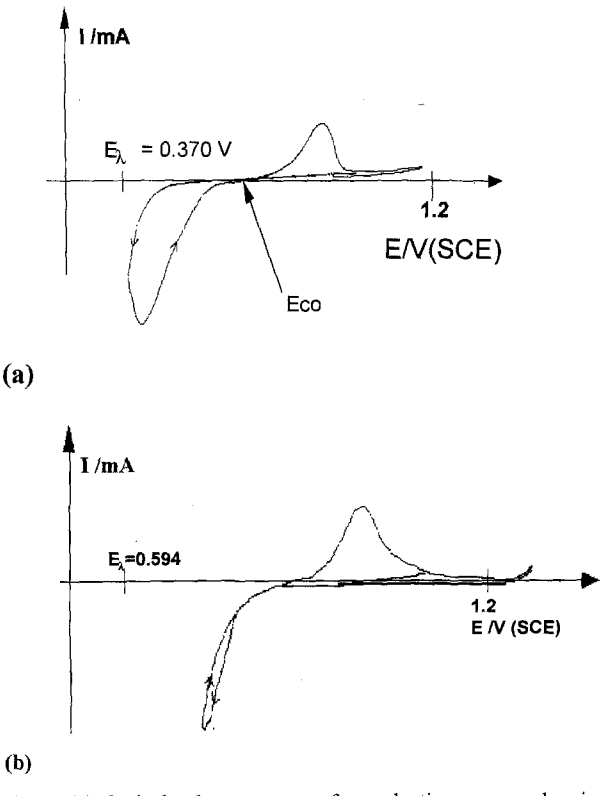

Fig. 2. (a) Typical voltammogram of a nucleation process showing the crossover potential (E_{co}) for the deposition of gold on GC. (b) Typical voltammogram for the deposition of gold on Pt where no crossover is observed. In both cases the switching potential was fixed to more anodic potentials than the reduction peak.

Table 1. Analysis of the gold nucleation process at 30 °C in an ammonia bath using chronoamperometric data

E /mV	$10^7 \times (i_m)^2 t_m$ /A cm^{-2}	$10^{-7} \times AN_o$ /sites cm^{-2} s^{-1}	$10^{-5} N_s$ /sites cm^{-2}	r /μm
350	0.847	1.09	19.0	4.09
300	0.952	1.14	16.9	4.33
280	0.939	1.13	17.8	4.23
250	0.985	2.55	26.6	3.45

Table 2. Analysis of the gold nucleation process at 40 °C in an ammonia bath using chronoamperometric data

E /mV	$10^7 \times (i_m)^2 t_m$ /A cm^{-2}	$10^{-7} \times AN_o$ /sites cm^{-2} s^{-1}	$10^{-5} N_s$ /sites cm^{-2}	r /μm
390	2.83	0.407	9.3	5.85
360	2.54	0.483	10.0	5.64
340	2.60	0.343	8.52	6.11
320	2.50	0.755	13.7	4.82

Fletcher theory [15, 16], it was concluded that the nuclei growth rate is independent of nucleation time within the potential range where the E_λ is studied. Therefore, the growth rate is charge transfer controlled and is determined only by the imposed potential for gold nucleation on GC. E_{co} corresponds to the standard potential of the system ($E^{\circ\prime}$). In this study a value of +0.59 V vs SCE was obtained, which agrees well with that calculated from the Pourbaix diagram for the $Au(NH_3)_2^+/Au(0)$ couple (+0.578 V at 25 °C) [6].

On the other hand, no cross-over is observed on Pt (Fig. 2(b)). This difference is probably due to the different overpotential required to form the first nuclei on surfaces of different nature. The overpotential required for nucleation on GC is much higher than that corresponding to deposition on platinum.

3.1.2. Chronoamperometric studies. Chronoamperometric studies at 25 °C were carried out within the potential range +0.6 to −0.3 V for experiments performed on GC. The transients obtained between +0.3 to −0.1 V and those obtained at potentials more cathodic than −0.22 V were found to follow a normal Cottrell decay. However, those transients obtained between −0.1 and −0.22 V showed an anomalous behaviour as shown in Fig. 3. This transient can be divided into three stages; in the first, the current decay is related to the charge of the double layer; then between 10 and 20 ms, the current becomes independent of time, and finally the current again follows a normal Cottrellian behaviour. The independence of current with respect to time observed between 10 ms and 20 ms indicates a process where nucleation is competing with adsorption. It is impor-

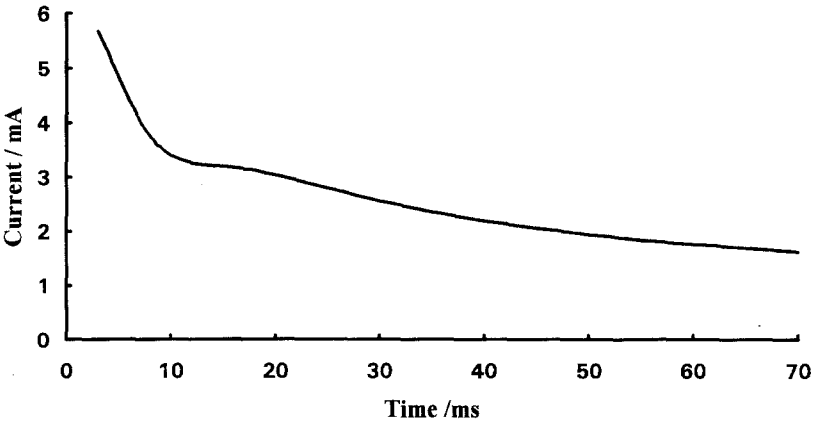

Fig. 3. Typical chronoamperogram for gold deposition on glassy carbon obtained at 25 °C, showing the characteristic shape for nucleation competing with an adsorption process. Potential step: −0.2 V vs SCE.

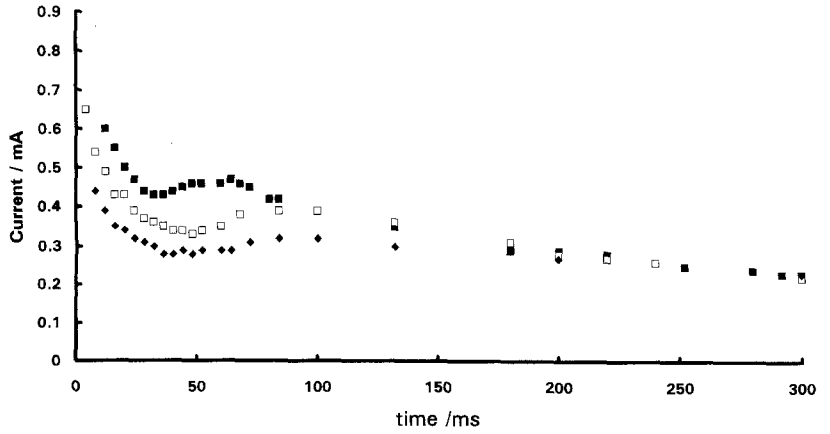

Fig. 4. Typical chronoamperograms for gold deposition on platinum obtained at 25 °C at different potential steps: (■) 450 mV; (□) 470 mV; (◆) 500 mV.

Table 3. Analysis of the gold nucleation process at 50 °C in an ammonia bath using chronoamperometric data

E /mV	$10^7 \times (i_m)^2 t_m$ /A cm^{-2}	$10^{-5} N_s$ /sites cm^{-2}	r /μm
350	2.10	1.50	14.56
340	2.01	3.00	10.30
300	2.01	5.60	7.53
280	2.11	7.78	6.39

tant to note that this type of process is accomplished in very short times (70 ms) and the current densities are high. This behaviour has been described by several authors [17–19] and corresponds to the reduction of chemical species adsorbed on the electrode surface.

Typical transients obtained for Pt within the potential range 0.5 to 0.45 V vs SCE are showed in Fig. 4. An increase in current is observed up to a maximum, which is typical behaviour for nucleation and crystal growth in a diffusion controlled process. The descending region in the transients has the form of a typical diffusion process.

To determine if the nucleation process is instantaneous or progressive, the rising portion of the chronoamperograms can be analysed by comparing the chronoamperometric curves to the nondimensional theoretical curves for instantaneous and progressive nucleation (Equations 1 and 2, respectively) [20].

$$(i/i_m)^2 = 1.9542\,(t/t_m)^{-1}\{1 - \exp[-1.2564\,(t/t_m)]\}^2 \quad (1)$$

$$(i/i_m)^2 = 1.2254\,(t/t_m)^{-1}\{1 - \exp[-2.3367\,(t/t_m)^2]\}^2 \quad (2)$$

where i_m is the maximum current density and t_m is the time at which i_m occurs. In the equations describing the nucleation phenomenon, currents are given as current densities. Comparison between experimental and theoretical curves is performed by plotting $(i/i_m)^2$ against t/t_m, the dimensionless current and time parameters.

Figure 5(a) and (b) show the experimental data compared to the dimensionless plots for instantaneous and progressive nucleation. The experimental

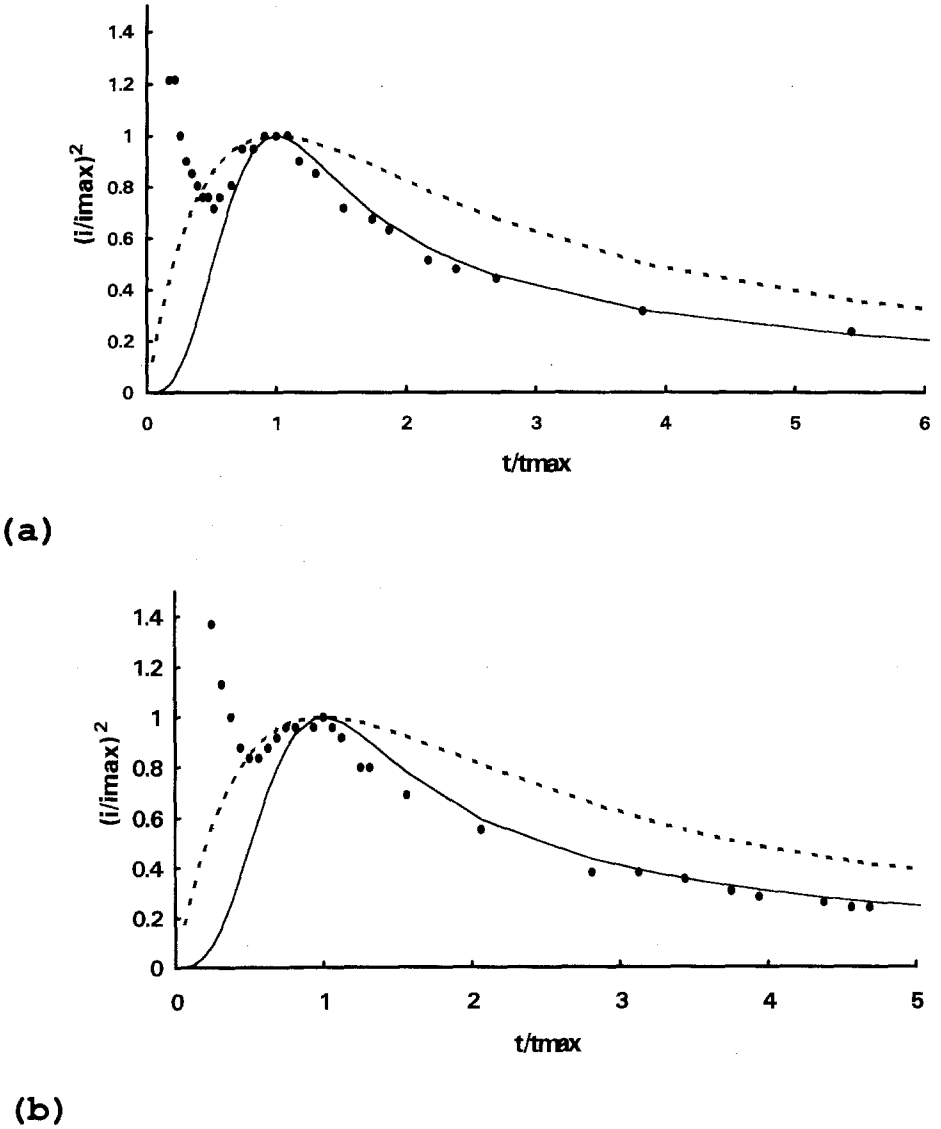

Fig. 5. Comparison of the experimental gold nucleation on Pt to the corresponding theoretical nucleation processes at 25 °C. (a) potential step: 500 mV; (b) potential step: 450 mV. (●) experimental; (——) theoretical progressive; (· · ·) theoretical instantaneous.

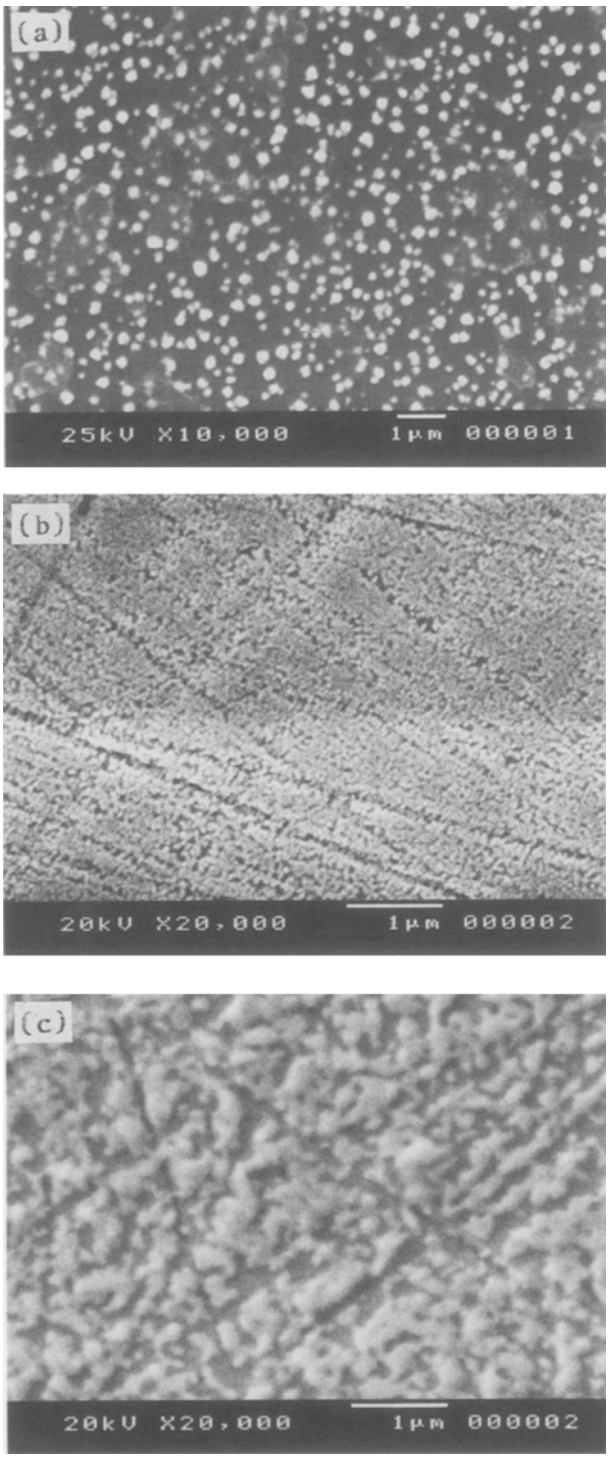

Fig. 6. SEM micrographs of electrodeposited gold from an ammoniacal solution at different potential steps and $t = 30$ s on different substrates. (a) GC potential step: −0.1 V vs SCE; (b) Pt potential step: 0.5 V vs SCE; (c) Pt potential step: 0.45 V vs SCE.

dimensionless plots are not described by either instantaneous or progressive theoretical curves. This is probably due to the influence of the competing adsorption process on the nucleation phenomena, an effect not considered in the theoretical dimensionless plots.

In the case of the nucleation of gold on platinum, the adsorption process is present; however, its influence on nuclei formation is smaller on this electrode material than on gold deposition on GC (compare Figs 3 and 4).

When the nucleation process cannot be classified as instantaneous or progressive, the current transient should be analysed using the method proposed by Scharifker and Mostany [20]. However, the experimental data available is insufficient to carry out this type of analysis.

3.1.3. Deposit morphology. The deposit morphology was examined by SEM. The deposits were grown potentiostatically at −0.1 V vs SCE on GC for 30 s; for the deposits on Pt, potential pulses where fixed at 0.5 and 0.45 V vs SCE with the same duration. Figure 6(a) shows that the deposit on the GC electrode is formed by hemispherical nuclei of different sizes. The time at the applied potential in this case corresponds to the descending region of the transient showed in Fig. 3; however coalescence of the nuclei does not occur. This behaviour may be explained considering that, in the vicinity of each nuclei, a circular region where formation of new nuclei is inhibited is formed. This region is called the exclusion zone [20]. Different morphology is obtained on Pt (Fig. 6(b)). Nuclei coalescence is observed and the size of the nuclei formed is much smaller than those formed on GC. An increase in the size of the nuclei is observed when the pulse is changed from 0.5 to 0.45 V (Fig. 6(c)).

3.2. *Influence of temperature*

The influence of temperature on the gold nucleation and growth was studied only on the GC electrode.

3.2.1. Cyclic voltammetry. Voltammetric studies were performed in the potential range −0.5 and +1.2 V at different temperatures (25, 30, 40 and 50 °C). The same voltammetric shape was observed at the four temperatures considered.

The influence of E_λ on E_{co} at the different temperatures was investigated. In these cases, when the temperature of the system was changed, it was found that E_{co} is independent of E_λ at each temperature. This means that in all cases nuclei growth is electron transfer controlled. It was also observed that E_{co} is anodically displaced with increasing temperature, meaning that less energy is required to perform the deposition at higher temperatures.

3.2.2. Chronoamperometry. The chronoamperometric studies at 25 °C show adsorption patterns described above. The adsorption patterns were not found for higher temperatures. Instead, transients exhibiting the classical shape for diffusion controlled nucleation were found in specific potential ranges, which are quite different for each temperature (roughly between +0.25 to +0.4 V). It is important to note that the current densities are much lower and the time required to reach the steady current density is longer, than those observed for the adsorption processes.

The type of nucleation was analyzed by comparing the chronoamperometric curves to the dimensionless

theoretical curves for instantaneous and progressive nucleation processes as above (Equations 1 and 2).

Experimental and theoretical data for a process at 40 °C are shown in Fig. 7(a). The plot for gold deposition on GC agrees well with the model for progressive nucleation. The same behaviour is observed at 30 °C. However, at 50 °C, (Fig. 7(b)), a different behaviour is observed. This deposition agrees better with the model for instantaneous nucleation.

The model proposed by Scharifker allows estimation of the nucleation type and the calculation of some of the related parameters. The electrocrystallization parameters are estimated using Equations 3 and 4 [22]:
For progressive nucleation:

$$N_s = (AN_o/2k'D)^{1/2} \quad (3)$$

For instantaneous nucleation:

$$N_s = 1.2564/t_m\pi kD \quad (4)$$

where A is the steady state nucleation rate constant *per site*, N_o is the number density of active sites and N_s is the nuclear number density observed at long times.

For the model of progressive nucleation, the following equations are valid:

$$i_m = 0.4615\,zFD^{3/4}c(k'AN_o)^{1/4} \quad (5)$$

$$t_m = (4.6733/AN_o\pi k'D)^{1/2} \quad (6)$$

$$k' = 4/3(8cM/\rho)^{1/2} \quad (7)$$

$$i_m^2 t_m = 0.2598\,(zFc)^2 D \quad (8)$$

For the model of instantaneous nucleation:

$$i_m = 0.6382\,zFDc(kN)^{1/2} \quad (9)$$

$$k = (8CM/\rho)^{1/2} \quad (10)$$

where D is the diffusion coefficient, c is the bulk

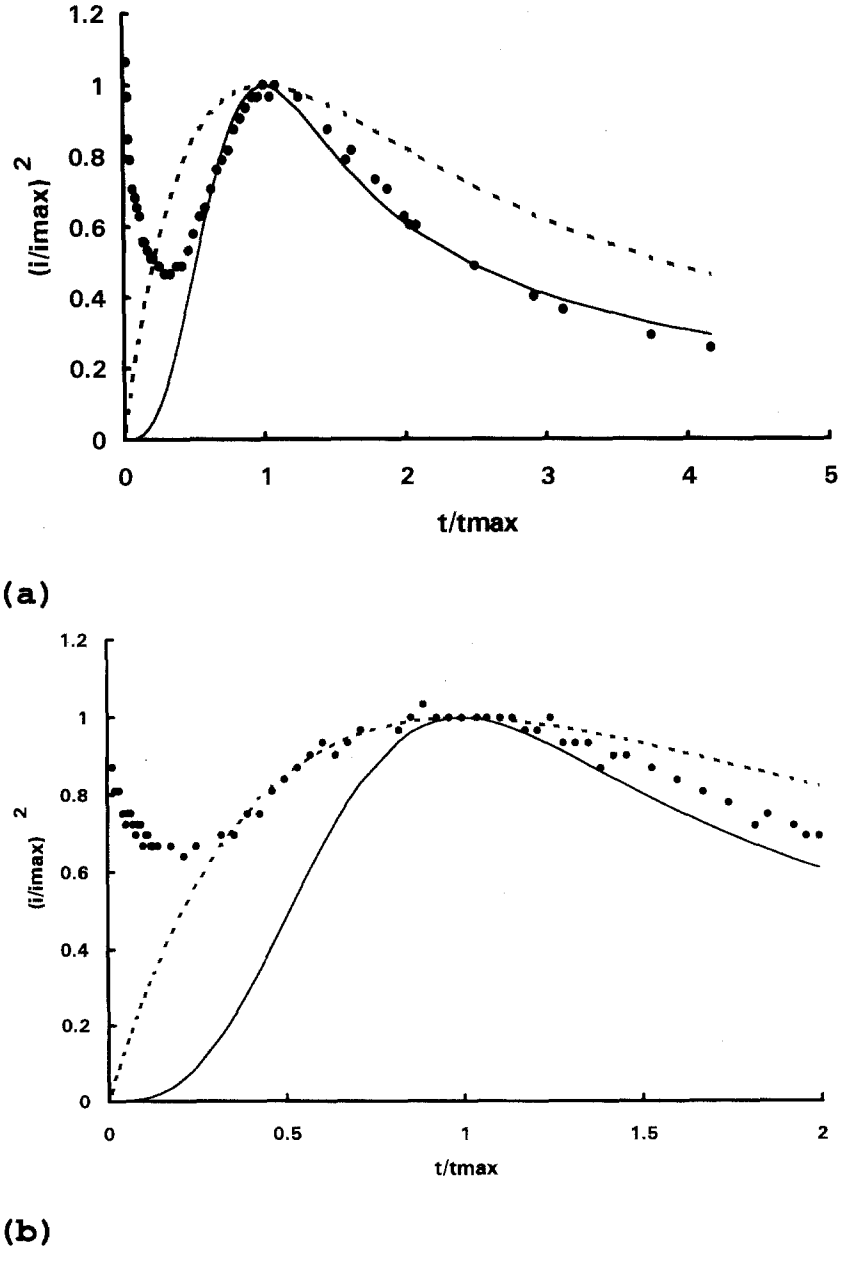

Fig. 7. Comparison of the experimental gold nucleation on GC to the corresponding theoretical nucleation processes. (a) Potential step: 0.32 V at 40 °C; (b) potential step: 0.34 V at 50 °C. (●) Experimental; (——) theoretical progressive; (· · ·) theoretical instantaneous.

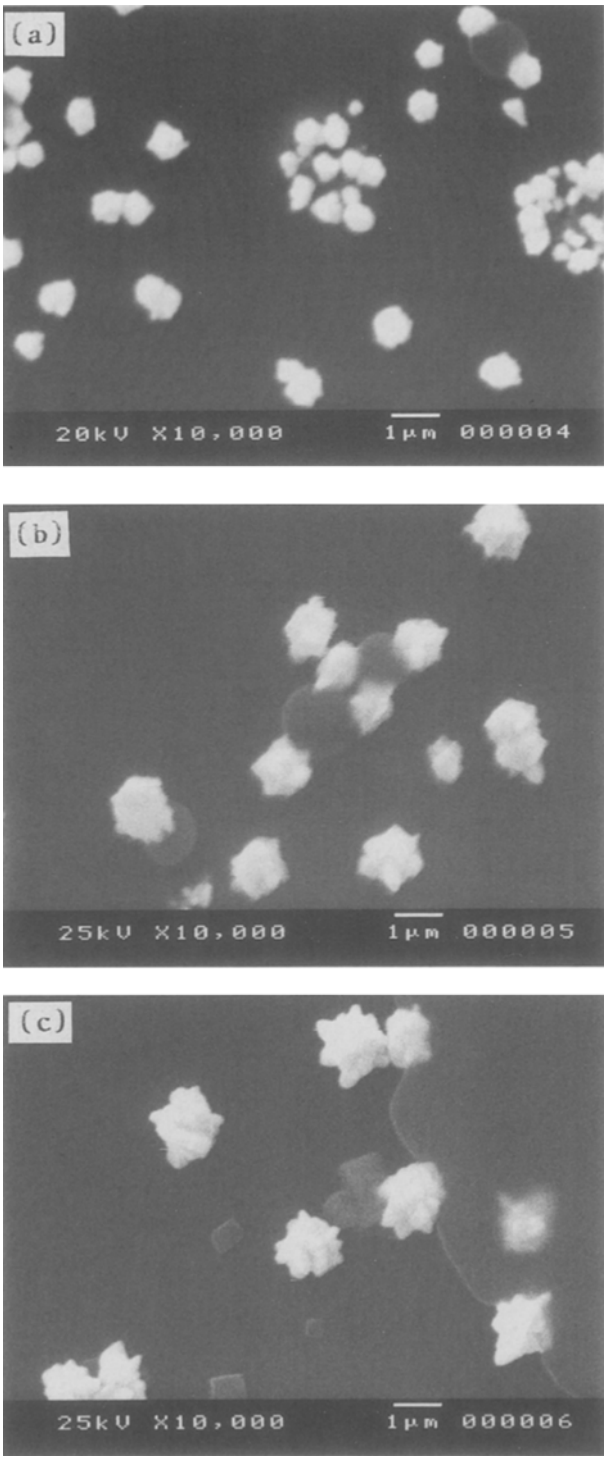

Fig. 8. SEM micrographs of electrodeposited gold from an ammoniacal solution at different temperatures on GC. Potential step: 0.36 V and $t = 20$ s. (a) 30 °C; (b) 40 °C; (c) 50 °C.

concentration, zF is the molar charge of the electrodepositing species, M and ρ are the molecular weight and density of the deposited materials, respectively. The other variables have their usual meaning [22].

The model for the potentiostatic transients, requires that the product $i_m^2 t_m$ be independent of the nucleation and growth rates [22]. Thus, at a given bulk concentration of electrodepositing species, it should not vary with the overpotential for which the surface concentration of gold ions is effectively zero.

3.2.3. Diffusion coefficient for $Au(NH_3)_2^+$. To obtain a better estimation of the nucleation parameters, a precise determination of the diffusion coefficient for the $Au(NH_3)_2^+$ species must be achieved. The calculation of the diffusion coefficient for electroactive species in a reaction where deposition onto the electrode surface phase takes place is difficult, because the modification of the electrode surface due to deposition produces distortions of the diffusional field. The rotating disc electrode chronoamperometry has been found to provide the most reliable results, and was the technique selected.

These experiments were performed at different temperatures (25, 30, 40 and 50 °C). The potential steps applied were in the range −0.25 to −0.40 V. From the transients at different rotation speeds, steady currents (i_l) were obtained. Plots of i_l against $\omega^{1/2}$ are linear and have zero intercept for this system. From the slopes of these lines, the diffusion coefficients of $Au(NH_3)_2^+$ were calculated at different temperatures using the Levich equation and have been reported elsewhere ($D_{25\,°C} = 2.59 \times 10^{-5}$ cm^2 s^{-1}; $D_{30\,°C} = 2.61 \times 10^{-5}$ cm^2 s^{-1}; $D_{40\,°C} = 3.03 \times 10^{-5}$ cm^2 s^{-1} and $D_{50\,°C} = 4.13 \times 10^{-5}$ cm^2 s^{-1}) [6].

3.2.4. Calculation of the nucleation parameters. The nucleation parameters calculated from the experimental results by means of equations 1 to 10 are reported in Tables 1 to 3. The product $i_m^2 t_m$ is constant, which allows application of the model described above.

In the temperature range considered, N_s was determined to be of order 10^6 to 10^5 nuclei per cm^2; values within this range have been found frequently at GC-water interfaces. It may be observed from the tables that N_s decreases with increasing temperature; this decrease is higher between 40 °C and 50 °C. Small variations of N_s with applied potential indicate that the imposed potential is used not only for activation of the sites (as proposed by the model), but also for the adsorption–desorption process, which is less important at higher temperatures. Thus, a larger variation of N_s with potential was observed at 50 °C.

Comparison of the tables shows a decrease in N_s and an increase in radius with increasing temperature. This agrees well with the change in the type of nucleation observed.

3.2.5. Morphology of the deposit. Deposits were grown on GC with a potential pulse of 0.36 V for 20 s. The deposit obtained at 30 °C is formed by hemispherical crystals of homogeneous size and a few crystals of smaller size (Fig. 8(a)). The same behaviour was observed at 40 °C (Fig. 8(b)). This behaviour corresponds to a progressive nucleation and growth process. At 50 °C crystals grow without new nuclei formation, indicating instantaneous nucleation (Fig. 8(c)).

At the potential steps (0.36 V) employed in this study, a time of 20 s corresponds to the descending part of the current–time transients obtained at the temperatures considered. It is important to note that

nucleus coalescence does not appear; this means that the maximum of the transients is not related to nuclei coalescence, but is related to the number of active sites and the coalescence of the diffusion layer of each nucleus.

X-ray analysis of the crystals produced shows that they are constituted exclusively of gold, and the presence of adsorbed chloride on the electrode surface free of gold nuclei.

4. Conclusions

Changes in the type of nucleation and morphology of the deposit are observed when the nature of the substrate is changed. The experimental results obtained at different temperatures were compared to the corresponding theoretical models. Temperature has a significant influence on this system, since it provokes a change in the nucleation process at high temperatures.

A change in the type of nucleation involves a change in the morphology and physical properties of the deposit; 'soft' deposits are obtained in the case of a progressive nucleation and 'hard' for an instantaneous nucleation. Eissaman [23] has reported that for gold reduction in cyanide medium the 'soft' or 'hard' nature of the deposit strongly depends on the adsorption of the electroactive species, due to modification of the nucleation rate. This difference can be demonstrated in cyanide baths, by adding traces of heavy metals that provoke depolarization effects [23]. However, the final gold deposit includes small amounts of those metals as impurities.

It is observed that, in the case of the ammoniacal medium, the morphology of the deposit may be modified from 'soft' to 'hard', by changing the temperature of the bath or the substrate onto which the electrodeposition is performed.

Acknowledgements

SEM micrographs were taken by F. Manríquez. This work was financially supported by CONACyT. G. Trejo thanks CONACyT for his scholarship and A. F. Gil thanks SRE (Mexico) for his scholarship.

References

[1] R. Raudsepp and R. Allgood, *Proceedings of the International Symposium on Gold Metallurgy*. Pergamon Press (1987) p. 87.
[2] M. T. Oropeza, *MSc. report*, Universidad Autónoma Metropolitana, México (1990).
[3] A. Serruya, B. R. Scharifker, I. González, M. T. Oropeza and M. Palomar-Pardavé, *J. Appl. Electrochem.*, **26** (1996) 451.
[4] M. Palomar-Pardavé, M. T. Ramírez, I. González, A. Serruya and B. R. Scharifker, *J. Electrochem. Soc.*, **143** (1996) 1551.
[5] X. Meng, *PhD dissertation*, SDSM&T, Rapid City SD, (1991) p. 228.
[6] G. Trejo, A. F. Gil and I. González, *J. Electrochem. Soc.* **142** (1995) 3404.
[7] L. H. Skibsted and J. Bjerrum, *Acta. Chem. Scan.* **A28** (1974) 764.
[8] *Idem, ibid.* **A28** (1974) 740.
[9] R. M. Smith and A. E. Martell, 'Critical Stability Constants', vol 4, Plenum Press, New York (1979).
[10] A. Rojas and I. González, *Anal. Chim. Acta* **187** (1986) 279.
[11] A. Rojas-Hernández, M. T. Ramírez, J. G. Ibáñez and I. González, *J. Electrochem. Soc.* **138** (1991) 365.
[12] A. Rojas-Hernández, M. T. Ramírez, I. González and J. G. Ibáñez, *Anal. Chim. Acta* **259** (1992) 95.
[13] A. Rojas-Hernández, M. T. Ramírez and I. González, *ibid.* **278** (1993) 321.
[14] A. Rojas-Hernández, M. T. Ramírez and I. González, *ibid.* **278** (1993) 335.
[15] S. Fletcher, *Electrochim. Acta* **28** (1983) 917.
[16] S. Fletcher and C. S. Halliday, *J. Electroanal. Chem.* **159** (1983) 167.
[17] W. J. Lorenz, E. Schmidt, G. Staikov and H. Bort, *Faraday Symp.* **12** (1977) 14.
[18] E. Bosco, *J. Chem. Soc. Faraday Trans.* **1** (1981) 1673.
[19] E. Bosco and S. K. Rangarajan, *J. Electroanal. Chem.* **134** (1982) 213.
[20] B. R. Scharifker and J. Mostany, *J. Electroanal. Chem.* **177** (1984) 13.
[21] B. R. Scharifker and G. Hills, *Electrochim. Acta* **28** (1983) 879.
[22] E. T. Eisenmann, *J. Electrochem. Soc.* **125** (1972) 717.